

# A spectral method for dispersive solutions of the nonlocal Sine-Gordon equation

A. Coclite<sup>a</sup>, L. Lopez<sup>b,\*</sup>, S. F. Pellegrino<sup>a</sup>

<sup>a</sup>*Dipartimento di Ingegneria Elettrica e dell'Informazione (DEI), Politecnico di Bari,  
Via Re David 200 – 70125 Bari, Italy*

<sup>b</sup>*Dipartimento di Matematica, Università degli Studi di Bari,  
Via Orabona 4 – 70125 Bari, Italy*

---

## Abstract

Motivated by the need for rigorous and reliable numerical tools for the analysis of peridynamic materials, the authors propose a model able to capture the dispersive features of nonlocal soliton-like solutions obtained by a peridynamic formulation of the Sine-Gordon equation. The analysis of the Cauchy problem associated to the peridynamic Sine-Gordon equation with local Neumann boundary condition is performed in this work through a spectral method on Chebyshev polynomial nodes joined with the Störmer-Verlet scheme for the time evolution. The choice for using the spectral method resides in the resulting reachable numerical accuracy, while, indeed, Chebyshev polynomials allow straightforward implementation of local boundary conditions. Several numerical experiments are proposed to thoroughly describe the ability of such scheme. Specifically, dispersive effects of the specific peridynamic kernel are demonstrated, while the internal energy behavior of the specified peridynamic operator is studied.

*Keywords:* Peridynamics, Nonlocal Sine-Gordon, Spectral Methods, Nonlocal Solitons, Numerical Methods.

*2020 MSC:* 74A70, 74B10, 70G70, 35Q70

---

\*Corresponding author

*Email addresses:* [alessandro.coclite@poliba.it](mailto:alessandro.coclite@poliba.it) (A. Coclite),  
[luciano.lopez@uniba.it](mailto:luciano.lopez@uniba.it) (L. Lopez), [sabrinafrancesca.pellegrino@poliba.it](mailto:sabrinafrancesca.pellegrino@poliba.it) (S. F. Pellegrino)

## Introduction

The Sine-Gordon Equation is a nonlinear partial differential equation that describes one-dimensional waves in a continuous media. It is often seen in various field theories, such as condensed matter physics and nonlinear optics. In the one-dimensional case, it is an example of a completely integrable system, meaning that the equation possesses an infinite number of conservation laws and that its solutions can be written in terms of spectral parameters through the inverse scattering method [1–4]. This property leads to exact solutions of the Sine-Gordon equation, known as solitons. Solitons are stable and localized nonlinear waves that retain their shape as they propagate. They have a crucial importance both in mathematics and physics since many physical systems present soliton-like behaviors. Solitons are widely seen in the theory but also exist as sound waves in nonlinear materials and as kinks or domain walls in nano-magnetic materials. The Sine-Gordon equation reads:

$$\partial_{tt}^2 u(x, t) - c^2 \partial_{xx}^2 u(x, t) + \sin(u(x, t)) = 0, \quad (0.1)$$

with  $x \in \mathbb{R}$  and  $t \in \mathbb{R}^+ \setminus \{0\}$  being the spatial and temporal coordinates, respectively,  $u(x, t)$  the displacement field and  $c$  the propagation speed. The choice of the nonlinear forcing term  $\sin(u(x, t))$  allows for the formation of solitons. Long-range interactions and memory effects can be introduced through an additive integral term to  $\sin(u(x, t))$  accounting for the global influence on the solution at a point [5–7]:

$$\partial_{tt}^2 u(x, t) - c^2 \partial_{xx}^2 u(x, t) + \sin(u(x, t)) - \int_{-\infty}^{\infty} S(x-y) \sin(u(y, t)) dy = 0. \quad (0.2)$$

$S(x-y)$  is a nonlocal kernel regulating the influence of the entire spatial domain on the wave dynamics. The specific form of such kernel defines range and character of nonlocal interactions. Eq.(0.2) often exhibits interesting and rich dynamics, and its solutions can involve the formation of various types of localized structures, including the so-called nonlocal solitons [8–10].

Indeed, nonlocality can be prescribed also for the wave internal response function  $\partial_{xx} u(x, t)$  by promoting the local Laplace operator to an integral operator. This theory is called peridynamics and corresponds to a non-local mechanics continuum theory extending local elasticity to long-range interactions thus accounting for material discontinuities, damages and failures [11–20]. The peridynamic Sine-Gordon equation reads:

$$\partial_{tt}^2 u(x, t) - \mathcal{L}(u(\cdot, t))(x) + \sin(u(x, t)) = 0, \quad (0.3)$$

where  $\mathcal{L}(u(\cdot, t))$  is the peridynamic kernel. As well-known, traditional continuum mechanics constitutive equations rely on spatial gradients of displacements and stresses. On the contrary, within peridynamic framework, the material internal energy is defined by integral (and often fractional) operators involving information from a region around a given point usually referred as *peridynamic horizon*. Moreover, the integro-differential nature of Eq. (0.3) depicts the material dynamics at several scales at the same time. This feature lies in its ability to capture the effects of small-scale features on the overall behavior of the solution [21–23]. The synergy between nonlocal differential equations and multiscale modeling enhances the ability to simulate and understand complex physical phenomena occurring in materials and systems with intricate structures and behaviors across multiple scales. In this context, any model can be generalized to a nonlocal model by rethinking the differential operator involved in the local formulation. Indeed, the physically soundness of the formulation as well as its convergence to the local original formulation is demanded to the constitutive choices made for  $\mathcal{L}(u(\cdot, t))(x)$ . The complexity of the peridynamic operator would often require the use of raffinate numerical tools for approximating the evolution of the system in time. In the last two decades the increasing interest in peridynamics grossly divided the researchers in two main directions: finite element models [24–29] and mesh-free methods [30–33] or quadrature methods [34]. Only in the very last years spectral methods [35–40] and boundary element methods [41] have been developed enlarging the range of suitable numerical tools. Indeed, due to the convergence properties of different numerical scheme, mesh-free and quadrature methods are commonly chosen when dealing with nonlinear kernels; on the contrary, spectral methods and boundary element methods are usually chosen for accurate numerical solutions of complex semilinear or linear peridynamics. As for finite elements discretization, the number of proposed schemes in literature is so large and so diverse that a main application is hard to find. Moreover, the specific formulation of a peridynamic equation, including the choice of the kernel function and the underlying assumptions, may vary based on the requirements of the specific application or material being studied. As the matter of facts, by combining some grandstanding ingredients such as, nonlocality, fractionality, nonlinearity and singularity, the ability of a specific peridynamic kernel is defined [42].

In this paper we consider the fractional one-dimensional kernel proposed

and discussed in [43]:

$$\mathcal{L}u(x, t) = \int_{B_\delta(x)} f(x-x', u(x, t)-u(x', t)) dx' = \int_{B_\delta(x)} \frac{u(x, t) - u(x', t)}{|x - x'|^{1+2\alpha}} dx', \quad (0.4)$$

with  $\alpha \in (0, 1)$  and  $B_\delta(x)$  being the interval centered on  $x$  by radius  $\delta$ . This choice is motivated under the following four physically-sound constitutive assumptions for the pairwise force interaction  $f : \mathbb{R} \times (\mathbb{R} \setminus \{0\}) \rightarrow \mathbb{R}$ :

- $f \in C^1(\mathbb{R} \times (\mathbb{R} \setminus \{0\}); \mathbb{R})$  ,
- $f(x-x', u(x)-u(x')) = f(x'-x, u(x)-u(x'))$  for every  $(x-x', u(\cdot, t)) \in \mathbb{R} \times (\mathbb{R} \setminus \{0\})$  ,
- $f(x-x', u(x)-u(x')) = -f(x'-x, u(x')-u(x))$  for every  $(x-x', u(\cdot, t)) \in \mathbb{R} \times (\mathbb{R} \setminus \{0\})$  ,
- there exists a function  $\Phi \in C^2(\mathbb{R} \times (\mathbb{R} \setminus \{0\}))$  such that  $\Phi = \nabla_u f$  .

Due to the choice made for the pairwise force interaction, the energy space is  $H^\alpha$  and  $\mathcal{L}u(x, t)$  corresponds to the censured- $\alpha$ -Laplacian ( $\alpha$  being the fractionality parameter). This formulation has been proven to converge to the local Laplace operator [43, 44]; in this light it represents the natural generalization of the local sine-Gordon equation.

The analysis of the evolutionary problem associated to Eq.(0.3) with local Neumann boundary condition is addressed here by adopting the spectral method approach on Chebyshev polynomials nodes while the temporal integration is demanded to the Störmer-Verlet scheme, thus returning a suitable, efficient and accurate computational tool [36, 37, 40]. This method is peculiarly suited for integral operator that can be expressed as convolution product so that preserving the computational properties of the Fast Fourier Transform (FFT) algorithm. Moreover, discretizing the spatial domain with trigonometric polynomials boundary conditions may be readily imposed [38, 39].

The paper is organized as follows. In Section 1 we present the evolutionary problem associated to the peridynamic Sine-Gordon equation and we prove the conservation of the energy of the model. In Section 2 we propose a spectral discretization for the evolutionary problem and prove the convergence of the solutions of the semidiscretized problem to the ones of the continuous problem. In Section 3 the full discretization of the semi-discrete problem is obtained by using the Störmer-Verlet scheme. Section 4 is devoted to the numerical simulations: in Section 4.1 we firstly critically



analyze strength and limitation of the proposed spectral method by validating the latter against a consolidated second-order finite difference scheme within several benchmark tests. Such tests include soliton-like solutions. Then, in Section 4.2 we demonstrate the presence of dispersive effects on the solution of the nonlocal evolutionary problem and, lastly, in Section 4.3 we experimentally study the energy behavior of the fully-discrete scheme. The numerical simulation shows a sort of *almost-preserving* property of the fully-discrete scheme proposed in the sense that unless a certain initial time in which the energy functional presents strong oscillations, then the behavior of the discretized energy oscillates around 1 with a one percent error. Conclusions and future outlines end the paper.

## 1. The model

We consider the nonlocal one-dimensional Sine-Gordon equation given by

$$\partial_{tt}^2 u(x, t) = \mathcal{L}u(x, t) - \sin(u(x, t)), \quad (1.1)$$

defined on a compact domain  $\Omega \subset \mathbb{R}$ , where  $\mathcal{L}$  is the integro-differential operator defined as

$$\mathcal{L}u(x, t) = \int_{B_\delta(x)} \frac{u(x, t) - u(x', t)}{|x - x'|^{1+2\alpha}} dx', \quad \alpha \in (0, 1), \quad (1.2)$$

where  $B_\delta(x)$  is the  $x$ -centered ball with radius  $\delta > 0$ , with initial conditions

$$u(x, 0) = u_0(x), \quad \partial_t u(x, 0) = v_0(x). \quad (1.3)$$

The well-posedness of the Cauchy problem (1.1)-(1.3) in the energy space and in the framework of hyper-elastic constitutive assumptions can be found in [43]. Therein it is also showed that the energy associated to (1.1) is given by

$$\begin{aligned} E[u](t) &= \frac{1}{2} \int_{\Omega} |\partial_t u(x, t)|^2 dx - \frac{1}{4} \int_{\Omega} \int_{B_\delta(x)} \frac{(u(x, t) - u(x', t))^2}{|x - x'|^{1+2\alpha}} dx' dx \\ &\quad - \int_{\Omega} (1 - \cos(u(x, t))) dx \end{aligned} \quad (1.4)$$

**Lemma 1.1** (Energy preserving property). *The energy's functional defined in (1.4) is preserved by time.*

*Proof.* We have

$$\begin{aligned}
\frac{d}{dt}E[u](t) &= \int_{\Omega} \partial_t u(x, t) \partial_{tt}^2 u(x, t) dx \\
&\quad - \frac{1}{2} \int_{\Omega} \int_{B_{\delta}(x)} \frac{(u(x, t) - u(x', t))}{|x - x'|^{1+2\alpha}} (\partial_t u(x, t) - \partial_t u(x', t)) dx' dx \\
&\quad + \int_{\Omega} \partial_t u(x, t) \sin(u(x, t)) dx \\
&= \underbrace{\int_{\Omega} \partial_t u(x, t) (\partial_{tt}^2 u(x, t) + \sin(u(x, t))) dx}_{=: I_1} \\
&\quad - \frac{1}{2} \underbrace{\int_{\Omega} \int_{B_{\delta}(x)} \frac{(u(x, t) - u(x', t))}{|x - x'|^{1+2\alpha}} \partial_t u(x, t) dx' dx}_{=: I_2} \\
&\quad + \frac{1}{2} \underbrace{\int_{\Omega} \int_{B_{\delta}(x)} \frac{(u(x, t) - u(x', t))}{|x - x'|^{1+2\alpha}} \partial_t u(x', t) dx' dx}_{=: I_3}.
\end{aligned} \tag{1.5}$$

We need to show that  $I_3 = -I_2$ . If we use the constitutive assumptions on the pair-wise force interaction function, by making a change of variables and rearranging terms in  $I_3$  we find

$$\begin{aligned}
I_3 &= \frac{1}{2} \int_{\Omega} \int_{B_{\delta}(0)} \frac{u(x, t) - u(x - x', t)}{|x'|^{1+2\alpha}} \partial_t u(x - x', t) dx' dx \\
&= \frac{1}{2} \int_{\Omega} \int_{B_{\delta}(0)} \frac{u(x, t) - u(x + x', t)}{|x'|^{1+2\alpha}} \partial_t u(x + x', t) dx' dx \\
&= -\frac{1}{2} \int_{\Omega} \int_{B_{\delta}(0)} \frac{u(x + x', t) - u(x, t)}{|x'|^{1+2\alpha}} \partial_t u(x + x', t) dx' dx \tag{1.6} \\
&= -\frac{1}{2} \int_{\Omega} \int_{B_{\delta}(x)} \frac{u(x, t) - u(x', t)}{|x - x'|^{1+2\alpha}} \partial_t u(x, t) dx' dx \\
&= -I_2.
\end{aligned}$$

Sustituting (1.6) into (1.5) and using (1.1) and the definition of the integral operator  $\mathcal{L}$  in (1.2), we get the claim.  $\square$

## 2. Spectral semi-discretization

Pseudo-spectral methods are often used to study nonlinear wave phenomena [45, 46]. They are based on the implementation of the fast-Fourier transform on equidistant collocation points and require the imposition of periodic boundary conditions. A different approach allowing to overcome the limitation of such boundary condition consists in considering the Chebyshev polynomials and the derivative matrix. Following this strategy, the nonlocal Sine-Gordon equation (1.1) can be discretized in space by using Chebyshev polynomials. The use of spectral methods allows us to obtain high accuracy in the profile of the solution and, moreover, this approach is typically used when the integral operator can be expressed in terms of convolution products [39, 38, 40]. Indeed, Chebyshev method can exploit the properties of the FFT algorithm to compute efficiently such products. Additionally, the choice of Chebyshev polynomials within the family of trigonometric polynomials allows us to impose more general boundary conditions.

The method consists in the approximation of the solution  $u(x, t)$  to (1.1) by a finite linear combination of Chebyshev polynomials of the first kind.

For simplicity we assume the spatial domain to be  $[-1, 1]$ , but a more general spatial interval can be considered by an affine transformation. Moreover we assume to have no-flux boundary conditions

$$\partial_x u(\pm 1, t) = 0. \quad (2.1)$$

We derive the semi-discrete model of (1.1) as follows.

Let  $N > 0$  be the total number of discretization points in the spatial domain  $\Omega = [-1, 1]$  and  $x_h = \cos(\pi h/N)$ ,  $h = 0, \dots, N$  be the Chebyshev Gauss-Lobatto (CGL) points. We also define  $\Omega_x = B_\delta(x) \cap [-1, 1]$ , for any  $x \in [-1, 1]$ , so that  $\Omega_0 = B_\delta(0) \cap [-1, 1]$ .

Then, if we set

$$k(x) = \frac{1}{|x|^{1+2\alpha}} \chi_{\Omega_0}(x), \quad (2.2)$$

where  $\chi_\Omega$  denotes the characteristic function which takes value 1 if  $x \in \Omega$  and value 0 otherwise, then we can rewrite equation (1.1) as follows

$$\partial_{tt}^2 u(x, t) = \beta u(x, t) - (k * u)(x, t) - \sin(u(x, t)), \quad (2.3)$$

where  $\beta = \int_{B_\delta(0)} k(s) ds$ .

We notice that  $\beta$  is well-defined because due to the nonlocal nature of the model, it does not allow self-interactions among material points and

as a consequence the integrand  $k$  is not discontinuous over the domain of integration. Hence, we can assume that the kernel  $k$  is uniformly bounded.

We look for an approximation of the solution  $u(x, t)$  in the form of a finite linear combination of Chebyshev polynomials  $T_n(x)$

$$u^N(x, t) = \sum_{n=0}^N \tilde{u}_n(t) T_n(x), \quad x \in \Omega, \quad t > 0, \quad (2.4)$$

where the coefficients  $\tilde{u}_n(t)$  represent the discrete Chebyshev coefficients given by

$$\tilde{u}_n = \frac{1}{\gamma_n} \sum_{h=0}^N u(x_h) T_n(x_h) w_h, \quad (2.5)$$

where  $\gamma_n$  is a normalization constant defined by

$$\gamma_n = \begin{cases} \pi & n = 0, N \\ \frac{\pi}{2} & n = 1, \dots, N-1 \end{cases} \quad (2.6)$$

and

$$w_h = \begin{cases} \frac{\pi}{2N} & h = 0, N \\ \frac{\pi}{N} & h = 1, \dots, N-1. \end{cases} \quad (2.7)$$

The presence of these constants is required to ensure the orthogonality property of the Chebyshev polynomials with respect to the weight function  $w(x) = 1/\sqrt{1-x^2}$ .

We substitute  $u$  by  $u^N$  into (2.3). Since Chebyshev transform, denoted here by  $\mathcal{F}$ , fulfills the same properties of Fourier transform, we can rewrite a convolution product in the physic space as a multiplication of the Chebyshev transform of each factor in the frequency space. Thus, on each interior collocation point  $x_h$ ,  $h = 1, \dots, N-1$ , equation (2.3) can be approximated as follows

$$\partial_{tt}^2 u^N(x_h, t) = \beta u^N(x_h, t) - \mathcal{F}^{-1}(\mathcal{F}(k) \mathcal{F}(u^N))(x_h, t) - \sin(u^N(x_h, t)). \quad (2.8)$$

In the same way we approximate the initial conditions in (1.3) by

$$u^N(x_h, 0) = u_0(x_h), \quad \partial_t u^N(x_h, 0) = v_0(x_h), \quad h = 0, \dots, N. \quad (2.9)$$

Following [47], in order to impose Neumann boundary conditions to the

discrete approximated solution

$$\partial_x u^N(x_0, t) = \partial_x u^N(x_N) = 0, \quad (2.10)$$

on each time level we have to solve the  $2 \times 2$  system

$$\begin{cases} d_{00}u^N(x_0, t) + d_{0N}u^N(x_N, t) &= -\sum_{h=1}^{N-1} d_{0h}u^N(x_h, t), \\ d_{NN}u^N(x_N, t) + d_{N0}u^N(x_0, t) &= -\sum_{h=1}^{N-1} d_{Nh}u^N(x_h, t), \end{cases} \quad (2.11)$$

where  $D = (d_{ij})$ ,  $i, j = 0, \dots, N$  is the matrix representing the spectral derivative at the CGL collocation points (an explicit formula for the component of  $D$  can be found in [48]). For readers' convenience, we remark that equations (2.11) basically represent the multiplication of the first row and the last row of the derivative matrix  $D$  by  $u^N$ . Indeed, the left-hand side refers to the derivative of  $u^N$  at the boundary meshpoints  $x_0$  and  $x_N$ .

We can prove the convergence of the semi-discrete scheme (2.8)-(2.9)-(2.10) in the framework of weighted Sobolev space  $H_w^s(\Omega)$ ,  $s \geq 1$ .

We start by introducing the functional setting under consideration. In what follows,  $C$  denotes a generic positive constant. We denote by  $(\cdot, \cdot)_w$  and  $\|\cdot\|_w$  the inner product and the norm of  $L_w^2(\Omega)$ , respectively, namely

$$(u, v)_w = \int_{\Omega} u(x)v(x)w(x) dx, \quad \|u\|_w^2 = (u, u)_w,$$

with  $w(x) = (\sqrt{1-x^2})^{-1}$ .

Let  $s > 0$ ,  $H_w^s(\Omega)$  be the weighted Sobolev space and  $X_s = \mathcal{C}^1(0, T; H_w^s(\Omega))$  be the space of all continuous functions in  $H_w^s(\Omega)$  whose distributional derivative is in  $H_w^s(\Omega)$ , with norm

$$\|u\|_{X_s}^2 = \max_{t \in [0, T]} \left( \|u(\cdot, t)\|_w^2 + \|\partial_t u(\cdot, t)\|_w^2 \right),$$

for any  $T > 0$ .

We introduce the space of Chebyshev polynomials of degree  $N$  as follows

$$S_N = \text{span} \{T_k(x) \mid -N \leq k \leq N\},$$

and we define the projection operator  $P_N : L_w^2(\Omega) \rightarrow S_N$  as

$$P_N u(x) = \sum_{|k| \leq N} \tilde{u}_k T_k(x).$$

It is such that for any  $u \in L_w^2(\Omega)$ , the following equality holds

$$(u - P_N u, \varphi)_w = 0, \quad \text{for every } \varphi \in S_N. \quad (2.12)$$

We have that the projector operator  $P_N$  commutes with derivatives in the distributional sense:

$$\partial_x^q P_N u = P_N \partial_x^q u, \quad \text{and} \quad \partial_t^q P_N u = P_N \partial_t^q u.$$

Then, spectral scheme (2.8)-(2.9)-(2.10) can be rewritten by using the projection  $P_N$  in the following way

$$\begin{aligned} \partial_{tt}^2 u^N &= P_N \mathcal{L}(u^N) - P_N \sin(u^N), \\ u^N(x, 0) &= P_N u_0(x), \quad \partial_t u^N(x, 0) = P_N v(x), \\ \partial_x u^N(\pm 1, t) &= 0, \end{aligned} \quad (2.13)$$

where  $u^N(x, t) \in S_N$  for every  $0 \leq t \leq T$ .

We recall the following lemma which is preliminary to our result.

**Lemma 2.1** (see [49]). *Let  $0 \leq \mu \leq s$ , if  $u \in H_w^s(\Omega)$ , then the following inequality holds*

$$\|u - P_N u\|_{H_w^\mu(\Omega)} \leq C N^{\mu-s} \|u\|_{H_w^s(\Omega)}, \quad (2.14)$$

for any positive constant  $C$ .

We can prove the following theorem.

**Theorem 2.2.** *Let  $s \geq 1$ , and assume  $u(x, t) \in X_s$  is the solution of the problem (1.1) with initial conditions  $u_0, v \in H_w^s(\Omega)$ , and  $u^N(x, t)$  is the solution of the semi-discrete scheme (2.13). Then, there exists a positive constant  $C = C(T)$ , which does not depend on  $N$ , such that*

$$\|u - u^N\|_{X_1} \leq C L(T) \left(\frac{1}{N}\right)^{s-1} \|u\|_{X_s}. \quad (2.15)$$

*Proof.* Let  $s \geq 1$ . Triangular inequality gives us

$$\|u - u^N\|_{X_1} \leq \|u - P_N u\|_{X_1} + \|P_N u - u^N\|_{X_1}. \quad (2.16)$$

Let we first focus on  $\|u - P_N u\|_{X_1}$ . Thanks to Lemma 2.1 we have

$$\|(u - P_N u)(\cdot, t)\|_{H_w^1(\Omega)} \leq C N^{1-s} \|u(\cdot, t)\|_{H_w^s(\Omega)},$$

and

$$\|\partial_t(u - P_N u)(\cdot, t)\|_{H_w^1(\Omega)} \leq CN^{1-s} \|\partial_t u(\cdot, t)\|_{H_w^s(\Omega)}.$$

Therefore,

$$\|u - P_N u\|_{X_1} \leq CN^{1-s} \|u\|_{X_s}. \quad (2.17)$$

We now estimate the term  $\|P_N u - u^N\|_{X_1}$ . We fix  $\varphi = \partial_t(P_N u - u^N) \in S_N$  as test function. Subtracting (2.13) from (1.1) and taking the inner product with the test function  $\varphi$ , we get

$$\begin{aligned} 0 &= \underbrace{\int_{\Omega} (\partial_{tt}^2 u(x, t) - \partial_{tt}^2 u^N(x, t)) \partial_t (P_N u(x, t) - u^N(x, t)) w(x) dx}_{=: I_1} \\ &\quad - \underbrace{\int_{\Omega} (\mathcal{L}(u(x, t)) - P_N \mathcal{L}(u^N(x, t))) \partial_t (P_N u(x, t) - u^N(x, t)) w(x) dx}_{=: I_2} \\ &\quad + \underbrace{\int_{\Omega} (\sin(u(x, t)) - P_N \sin(u^N(x, t))) \partial_t (P_N u(x, t) - u^N(x, t)) w(x) dx}_{=: I_3}. \end{aligned} \quad (2.18)$$

We focus on  $I_1$ . The orthogonal condition (2.12) implies that

$$\int_{\Omega} (\partial_{tt}^2 u(x, t) - P_N \partial_{tt}^2 u(x, t)) \partial_t (P_N u(x, t) - u^N(x, t)) w(x) dx = 0.$$

Thus,

$$\begin{aligned} I_1 &= \int_{\Omega} (\partial_{tt}^2 u(x, t) - P_N \partial_{tt}^2 u(x, t)) \partial_t (P_N u(x, t) - u^N(x, t)) w(x) dx \\ &\quad + \int_{\Omega} (P_N \partial_{tt}^2 u(x, t) - \partial_{tt}^2 u^N(x, t)) \partial_t (P_N u(x, t) - u^N(x, t)) w(x) dx \\ &= \frac{1}{2} \frac{d}{dt} \|\partial_t(P_N u - u^N)(\cdot, t)\|_{H_w^1(\Omega)}^2. \end{aligned} \quad (2.19)$$

Thanks to (2.12), we have

$$\int_{\Omega} (\mathcal{L}(u^N(x, t)) - P_N \mathcal{L}(u^N(x, t))) \partial_t (P_N u(x, t) - u^N(x, t)) w(x) dx = 0.$$

Thus, since  $k \in L^\infty(\Omega)$ , using the Cauchy's inequality, we have

$$\begin{aligned}
I_2 &= \int_{\Omega} (\mathcal{L}(u(x, t)) - \mathcal{L}(u^N(x, t))) \partial_t (P_N u(x, t) - u^N(x, t)) w(x) dx \\
&= \int_{\Omega} \int_{\Omega_x} k(x' - x) (u(x', t) - u(x, t)) \partial_t (P_N u(x, t) - u^N(x, t)) w(x) dx' dx \\
&\quad - \int_{\Omega} \int_{\Omega_x} k(x' - x) (u^N(x', t) - u^N(x, t)) \partial_t (P_N u(x, t) - u^N(x, t)) w(x) dx' dx \\
&\leq \int_{\Omega} \int_{\Omega_x} k(x' - x) |u(x', t) - u^N(x', t)| \partial_t (P_N u(x, t) - u^N(x, t)) w(x) dx' dx \\
&\quad + \int_{\Omega} \int_{\Omega_x} k(x' - x) |u(x, t) - u^N(x, t)| \partial_t (P_N u(x, t) - u^N(x, t)) w(x) dx' dx \\
&\leq \left( \frac{\beta}{2} + \|k\|_{L^\infty(\Omega)} \right) \left( \|(u - u^N)(\cdot, t)\|_{H_w^1(\Omega)}^2 + \|\partial_t(P_N u - u^N)(\cdot, t)\|_{H_w^1(\Omega)}^2 \right).
\end{aligned} \tag{2.20}$$

Moreover, the orthogonality condition (2.12) ensures that

$$\int_{\Omega} (\sin(u^N(x, t)) - P_N \sin(u^N(x, t))) \partial_t (P_N u(x, t) - u^N(x, t)) w(x) dx = 0.$$

Therefore, due to the uniformly Lipschitzianity of the loading term and the Cauchy's inequality, we find

$$\begin{aligned}
I_3 &= \int_{\Omega} (\sin(u(x, t)) - P_N \sin(u^N(x, t))) \partial_t (P_N u(x, t) - u^N(x, t)) w(x) dx \\
&= \int_{\Omega} (\sin(u(x, t)) - \sin(u^N(x, t))) \partial_t (P_N u(x, t) - u^N(x, t)) w(x) dx \\
&\leq \frac{1}{2} \left( \|(u - u^N)(\cdot, t)\|_{H_w^1(\Omega)}^2 + \|\partial_t(P_N u - u^N)(\cdot, t)\|_{H_w^1(\Omega)}^2 \right).
\end{aligned} \tag{2.21}$$

We substitute (2.19), (2.20) and (2.21) in (2.18) and we obtain

$$\frac{1}{2} \frac{d}{dt} \|\partial_t(P_N u - u^N)(\cdot, t)\|_{H_w^1(\Omega)}^2 \leq C \|(u - u^N)(\cdot, t)\|_{H_w^1(\Omega)}^2 + C \|\partial_t(P_N u - u^N)(\cdot, t)\|_{H_w^1(\Omega)}^2. \tag{2.22}$$



We add to both sides of equation (2.22) the term

$$\frac{1}{2} \frac{d}{dt} \left\| (P_N u - u^N)(\cdot, t) \right\|_{H_w^1(\Omega)}^2 = \int_{\Omega} (P_N u(x, t) - u^N(x, t)) \partial_t (P_N u(x, t) - u^N(x, t)) w(x) dx,$$

then, we find

$$\begin{aligned} & \frac{d}{dt} \left( \left\| \partial_t (P_N u - u^N)(\cdot, t) \right\|_{H_w^1(\Omega)}^2 + \left\| (P_N u - u^N)(\cdot, t) \right\|_{H_w^1(\Omega)}^2 \right) \\ & \leq C \left( \left\| \partial_t (P_N u - u^N)(\cdot, t) \right\|_{H_w^1(\Omega)}^2 + \left\| (P_N u - u^N)(\cdot, t) \right\|_{H_w^1(\Omega)}^2 + \left\| (u - P_N u)(\cdot, t) \right\|_{H_w^1(\Omega)}^2 \right). \end{aligned}$$

Since  $\left\| \partial_t (P_N u - u^N)(\cdot, 0) \right\|_{H_w^1(\Omega)} = 0$  and  $\left\| (P_N u - u^N)(\cdot, 0) \right\|_{H_w^1(\Omega)} = 0$ , we can apply Lemma 2.1 and Gronwall's inequality obtaining

$$\begin{aligned} & \left( \left\| \partial_t (P_N u - u^N)(\cdot, t) \right\|_{H_w^1(\Omega)}^2 + \left\| (P_N u - u^N)(\cdot, t) \right\|_{H_w^1(\Omega)}^2 \right) \\ & \leq \int_0^t e^{C(t-\tau)} \left\| (u - P_N u)(\cdot, \tau) \right\|_{H_w^1(\Omega)}^2 d\tau \\ & \leq C(T) N^{2-2s} \int_0^t \left\| u(\cdot, \tau) \right\|_{H_w^1(\Omega)}^2 d\tau. \end{aligned}$$

Hence,

$$\left\| P_N u - u^N \right\|_{X_1} \leq C(T) N^{1-s} \|u\|_{X_s}. \quad (2.23)$$

Finally, using (2.17) and (2.23) in (2.16), we get the claim.  $\square$

### 3. The fully discrete scheme

The semi-discrete nonlocal formulation of Sine-Gordon equation in (2.8) can be integrated in time by using explicit forward and backward difference techniques. Störmer-Verlet method consists in a symplectic semi-implicit centered second-order finite difference scheme deeply used in the context of continuum mechanics and elastodynamics.

Let  $N_T > 0$  be the total number of time steps and  $\{t_s\}_{s=0}^{N_T}$  be a uniform partition of the computational interval  $[0, T]$ , with  $t_s = s\Delta t$  and  $\Delta t = \frac{T}{N_T}$ .

If we denote by

$$\mathcal{L}(u^N(\cdot, t))(x_h) = \beta u^N(x_h, t) - \mathcal{F}^{-1}(\mathcal{F}(k)\mathcal{F}(u^N))(x_h, t) \quad (3.1)$$

the spectral discretization of the nonlocal operator  $\mathcal{L}$  at the collocation

points  $x_h$ ,  $h = 0, \dots, N$ , then the semi-discrete scheme (2.8) can be compactly written as

$$\partial_{tt}^2 u^N(x_h, t) = \mathcal{L}(u^N(x_h, t)) - \sin(u^N(x_h, t)), \quad h = 0, \dots, N. \quad (3.2)$$

We set  $U_h^{N,s} = u^N(x_h, t_s)$  the approximation of the solution at the node  $x_h$  and at the discrete time  $t_s$ , for  $h = 0, \dots, N$  and  $s = 0, \dots, N_T$  and we denote  $V_h^{N,s} = (U_h^{N,s})'$ , then the Störmer-Verlet scheme for the system (3.2) is given by

$$\begin{cases} U_h^{N,s+1} = U_h^{N,s} + \Delta t \left( V_h^{N,s} + \frac{\Delta t}{2} \mathcal{L}(U_h^{N,s}) - \frac{\Delta t}{2} \sin(U_h^{N,s}) \right), \\ V_h^{N,s+1} = V_h^{N,s} + \frac{\Delta t}{2} \left( \mathcal{L}(U_h^{N,s}) - \sin(U_h^{N,s}) + \mathcal{L}(U_h^{N,s+1}) - \sin(U_h^{N,s+1}) \right), \end{cases} \quad (3.3)$$

for  $h = 0, \dots, N$  and  $s = 0, \dots, N_T$ .

#### 4. Numerical experiments

In this section we perform several simulations in order to study the properties of the solution of the model. The first test provides a validation of the spectral method by making a comparison between the solution obtained by Chebyshev method with the solution obtained by implementing a centered second order finite difference scheme. Then we show the dispersive effects due to the nonlocality in the profile of soliton-type solutions. Finally, we point out the energy behavior of the fully-discrete scheme by showing that, despite the continuous energy functional is preserved over time, the proposed fully-discrete scheme can be considered *almost-energy preserving*, in the sense that after certain initial oscillations, the energy functional recovers an averaged constant value.

##### 4.1. Test 1: Validation of the performance of the spectral method

In order to show that the spectral method approximates the correct solution, we make a comparison between the solution provided by the proposed Chebyshev method and the solution found by the implementation of a finite difference discretization. The latter corresponding to a centered second-ordered scheme in time explicitly combined with the trapezoidal rule approximation of the operator  $\mathcal{L}u(x, t)$ . We choose  $u_{0,1}(x) = 0$  and  $v_{0,1}(x) = 4 \left( \sqrt{1 - c^2} \cosh(x/\sqrt{1 - c^2}) \right)^{-1}$  as initial conditions, with  $c = 0.999$ . We fix  $\alpha = 0.4$  as parameter of the integral operator  $\mathcal{L}$  defined in (0.4) and

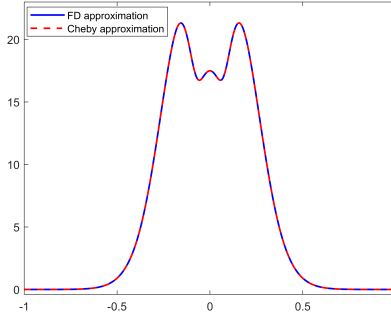


Figure 1: With reference to Section 4.1, the comparison between the approximated solution computed by spectral method with the one obtained by finite different discretization at time  $t = 1$  with initial conditions  $u_{0,1}(x)$  and  $v_{0,1}(x)$ . The parameters for the simulation are  $N = 400$ ,  $N_T = 800$ , the horizon is  $\delta = 0.2$  and  $\alpha = 0.4$ .

$\delta = 0.2$  as horizon. In Figure 1, we can observe a good agreement between the two numerical solutions.

In Figure 2 we show the comparison between the solution obtained by spectral method and finite difference method corresponding to the initial conditions  $u_{0,2}(x) = 4 \arctan\left(e^{\frac{x}{\sqrt{1-c^2}}}\right)$  and  $v_{0,2}(x) = -2c \frac{\operatorname{sech}\left(\frac{x}{\sqrt{1-c^2}}\right)}{\sqrt{1-c^2}}$ , with  $c = 0.999$ .

With reference to the solution corresponding to the initial conditions  $u_{0,2}(x)$  and  $v_{0,2}(x)$ , we also provide a convergence analysis of the proposed spectral scheme. We define the relative  $L^2$ -error as follows

$$Error_2 [u^N] (t) = \frac{\sum_{h=1}^N |u^N(x_h, t) - u^*(x_h, t)|^2}{\sum_{h=1}^N |u^*(x_h, t)|^2},$$

where  $u^*$  represents the reference solution obtained by using the finite difference scheme with  $N = 1600$ . Starting from the relative  $L^2$ -error, we can compute the convergence rate by looking for the slope of the line that best fit in the sense of least square the logarithm of the data.

Table 1 and Figure 3 depict the relative  $L^2$ -error and the convergence rate obtained by using the finite difference scheme and the proposed spectral method as the total number of spatial discretization points increases.

We can observe a gain in terms of convergence rate when a spectral method is applied.

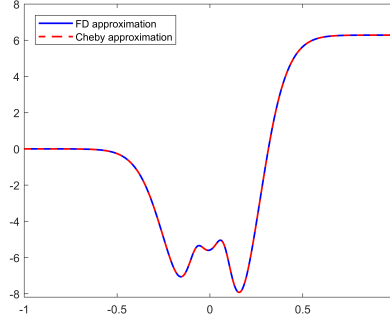


Figure 2: With reference to Section 4.1, the comparison between the approximated solution computed by spectral method with the one obtained by finite different discretization at time  $t = 1$  with initial conditions  $u_{0,2}(x)$  and  $v_{0,2}(x)$ . The parameters for the simulation are  $N = 400$ ,  $\Delta t = 8/N_T$ ,  $N_T = 800$ ,  $\delta = 0.2$  and  $\alpha = 0.4$ .

$N$	Finite Difference method		Chebyshev method	
	error	conv. rate	error	conv. rate
100	$2.1336 \times 10^{-3}$	—	$1.3600 \times 10^{-3}$	—
200	$4.7141 \times 10^{-4}$	2.1625	$1.9584 \times 10^{-4}$	27757
400	$1.0768 \times 10^{-4}$	2.1426	$7.1261 \times 10^{-6}$	3.7670
800	$1.8644 \times 10^{-5}$	2.2551	$3.8717 \times 10^{-7}$	3.9945

Table 1: With reference to Section 4.1, the relative error related to the initial conditions  $u_{0,2}(x)$  and  $v_{0,2}(x)$ , at time  $t = 2$  as function of the total number of discretization points.

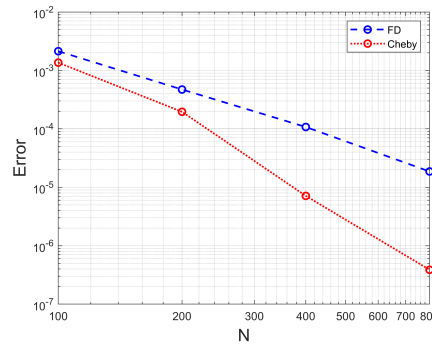
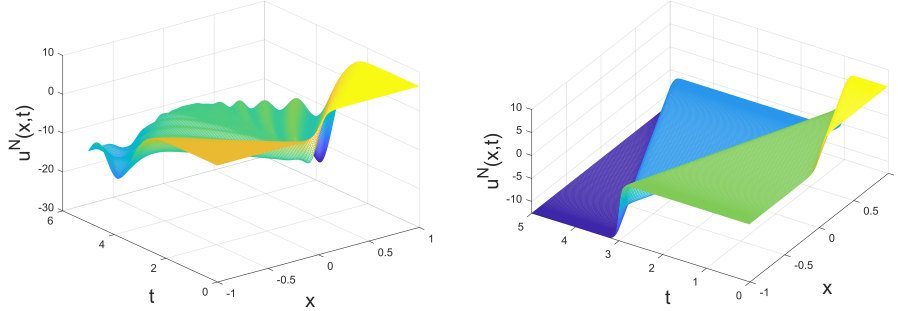


Figure 3: With reference to Section 4.1, the comparison between the relative error obtained with the two considered methods in the logarithmic scale.



The evolution of a kink soliton in the nonlocal model. The evolution of a kink soliton in the classical Sine-Gordon equation.

Figure 4: With reference to Section 4.2: the comparison between kink-type solitons in the nonlocal model and in the classical Sine-Gordon model. The parameters for the simulation are  $\delta = 0.2$ ,  $N = 200$ ,  $\alpha = 0.4$ , and  $N_T = 400$ .

#### 4.2. Test 2: The dispersive effects of the nonlocal model in soliton-type solutions

Due to the presence of long-range interactions, solutions of (1.1) are characterized by a dispersive behavior. As a consequence, soliton-type solutions lose the property to be travelling waves with constant velocity and shape-preserving profile and show the appearance of an oscillatory behavior, whose phase depends on the size of the horizon.

The nonlocal kink solution is compared with the classical one in Figure 4, where we can observe the evolution of the solution subject to the following initial conditions

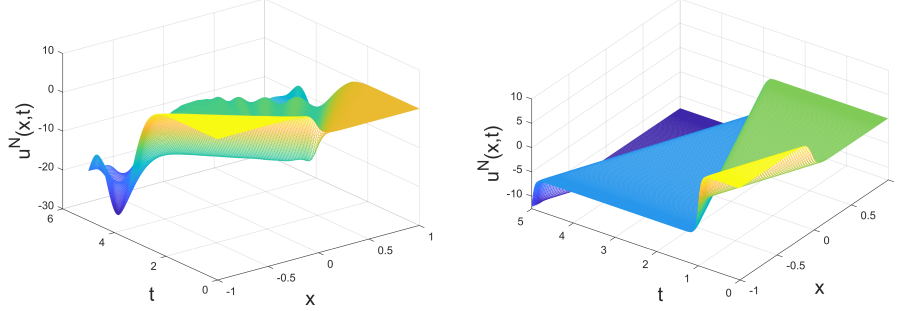
$$u_0(x) = 4 \arctan \left( e^{\frac{x}{\sqrt{1-c^2}}} \right),$$

$$v_0(x) = -2c \frac{\operatorname{sech} \left( \frac{x}{\sqrt{1-c^2}} \right)}{\sqrt{1-c^2}},$$

with velocity  $c = .999$ .

A comparison between antikink solutions is shown in Figure 5. The initial conditions for this test are

$$u_0(x) = 4 \arctan \left( e^{\frac{-x}{\sqrt{1-c^2}}} \right),$$



The evolution of a antikink soliton in the non-local model.

The evolution of a antikink soliton in the classical Sine-Gordon equation.

Figure 5: With reference to Section 4.2: the comparison between antikink-type solitons in the nonlocal model and in the classical Sine-Gordon model. The parameters for the simulation are  $\delta = 0.2$ ,  $N = 200$ ,  $\alpha = 0.4$ , and  $\Delta t = 8/N_T$ ,  $N_T = 400$ .

$$v_0(x) = -2c \frac{\operatorname{sech}\left(\frac{x}{\sqrt{1-c^2}}\right)}{\sqrt{1-c^2}},$$

with  $c = 0.999$ .

Figures 6 and 7 provide a comparison between local and nonlocal models in the case of a collision between two kink-type solitons or a collision between a kink and an antikink soliton, respectively. The initial conditions for these simulations are respectively

$$u_0(x) = 4 \arctan\left(c \sinh \frac{x}{\sqrt{1-c^2}}\right),$$

$$v_0(x) = 0,$$

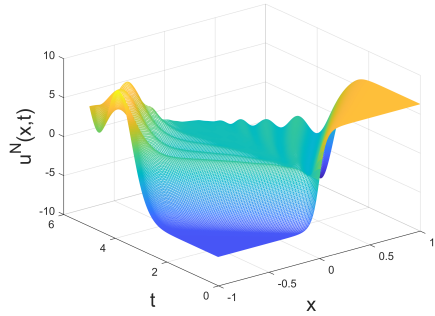
and

$$u_0(x) = 0,$$

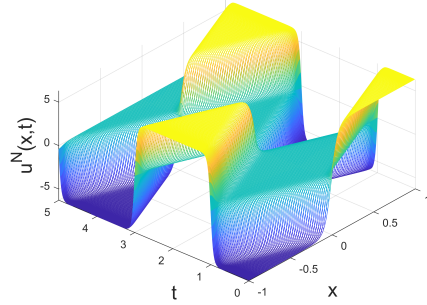
$$v_0(x) = \frac{4}{\sqrt{1-c^2} \cosh\left(\frac{x}{\sqrt{1-c^2}}\right)},$$

with  $c = 0.999$ .

Finally, the same dispersive effects can be observed even in the behavior of a breather solution as shown in Figure 8. In this case the initial conditions

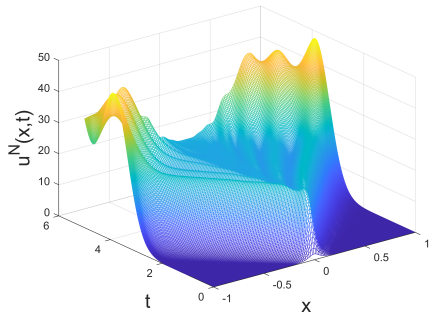


The evolution of a collision of two kink solitons in the nonlocal model.

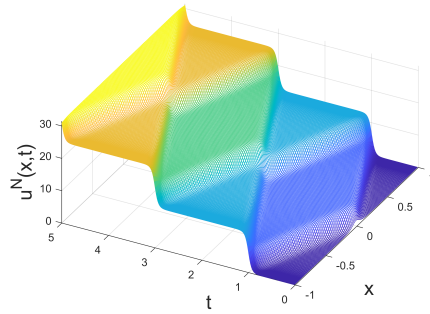


The evolution of a collision of two kink solitons in the classical Sine-Gordon equation.

Figure 6: With reference to Section 4.2: the comparison between the behavior of a collision of two kink-type solitons in the nonlocal model and in the classical Sine-Gordon model. The parameters for the simulation are  $\delta = 0.2$ ,  $N = 200$ ,  $\alpha = 0.4$ , and  $\Delta t = 8/N_T$ ,  $N_T = 400$ .

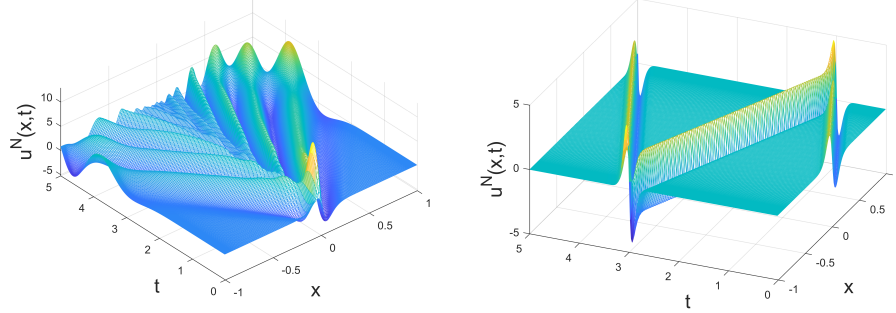


The evolution of a collision of a kink soliton with an antikink soliton in the nonlocal model.



The evolution of a collision of a kink soliton with an antikink soliton in the classical Sine-Gordon equation.

Figure 7: With reference to Section 4.2: the comparison between the behavior of a collision of kink-type soliton with an antikink-type soliton in the nonlocal model and in the classical Sine-Gordon model. The parameters for the simulation are  $\delta = 0.2$ ,  $N = 200$ ,  $\alpha = 0.4$ , and  $\Delta t = 8/N_T$ ,  $N_T = 400$ .



The evolution of a breather soliton in the non-local model. The evolution of a breather soliton in the classical Sine-Gordon equation.

Figure 8: With reference to Section 4.2: the comparison between the behavior of a breather-type soliton in the nonlocal model and in the classical Sine-Gordon model. The parameters for the simulation are  $\delta = 0.2$ ,  $N = 200$ ,  $\alpha = 0.4$ , and  $\Delta t = 8/N_T$ ,  $N_T = 400$ .

for the simulation are

$$u_0(x) = 4 \arctan \left( \frac{\sqrt{1-w^2} \sin \left( -\frac{cwx}{\sqrt{1-c^2}} \right)}{w \cosh \left( \frac{x\sqrt{1-w^2}}{\sqrt{1-c^2}} \right)} \right),$$

$$v_0(x) = 4w \frac{\sqrt{1-w^2}}{\sqrt{1-c^2}} \left( \frac{w \cos \left( -\frac{cwx}{\sqrt{1-c^2}} \right) \cosh \left( \frac{x\sqrt{1-w^2}}{\sqrt{1-c^2}} \right) + c\sqrt{1-w^2} \sin \left( -\frac{cwx}{\sqrt{1-c^2}} \right) \sinh \left( \frac{x\sqrt{1-w^2}}{\sqrt{1-c^2}} \right)}{w^2 \cosh^2 \left( \frac{x\sqrt{1-w^2}}{\sqrt{1-c^2}} \right) + (1-w^2) \sin^2 \left( -\frac{cwx}{\sqrt{1-c^2}} \right)} \right),$$

with  $c = 0.999$  and  $w = 0.4$ . In all shown cases, due to the dispersive effects, we can also observe a time delay in the soliton waves to reach the boundaries with respect to the local soliton waves.

#### 4.3. Test 3: The energy behavior of the fully-discrete scheme

The aim of the test is to check the behavior of the discrete energy functional associated to the proposed fully-discrete scheme. We take  $u_0(x) = e^{-x^2/0.002}$ ,  $v_0(x) = 0$ , as initial conditions and we fix the parameters of the model as  $\delta = 0.2$ ,  $\alpha = 0.4$  and  $N = 800$  and  $\Delta t = 10^{-4}$ . In Figure 9, we show the behavior of the distribution in time of  $E(t)/E(0)$ . It is clearly not constant, but oscillates around 1. Due to this, we refer to the proposed model as *almost-energy preserving* in time, in the sense that, although there are oscillations in the behavior of the discretized energy, their amplitude is such as to maintain the oscillations around one with an error of one percent except for the first instants of time. The reasons of such behavior need to



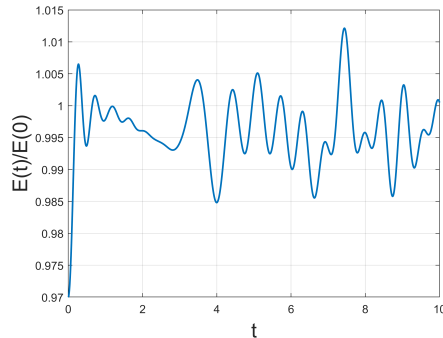


Figure 9: With reference to Section 4.3, the behavior of the energy functional.

be further investigated: it could be related to the fact that even if Störmer-Verlet scheme is a symplectic semi-implicit second-order integrator, it does not allow to maintain, in general, the energy-preserving property when applied to nonlinear problems, as shown for instance in [50, 51].

### Conclusive Remarks

A spectral method based on the Chebyshev nodes spatial discretization for the Cauchy problem related to the evolution of the peridynamic Sine-Gordon equation has been studied in this work. The consistency of such discretization has been rigorously proved and various numerical experiments have clarified strength and limitations of the proposed model. Specifically, the proposed model has been validated against a second order centered finite-difference scheme by comparing the evolution in time of several nonlocal soliton-type solutions. Lastly, dispersive effects as well the behavior of the energy functional of the specific peridynamic kernel have been experimentally showed.

### Acknowledgments

The authors thank the anonymous referees for their helpful and constructive remarks that have contributed to significantly improve the original manuscript. AC, LL, and SFP are members of Gruppo Nazionale per il Calcolo Scientifico (GNCS) of the Istituto Nazionale di Alta Matematica (INdAM). This work was partially supported by:

- Research Project of National Relevance “Evolution problems involving interacting scales” granted by the Italian Ministry of Education, University and Research (MUR Prin 2022, project code 2022M9BKBC, Grant No. CUP D53D23005880006);
- Research Project of National Relevance “Mathematical Modeling of Biodiversity in the Mediterranean sea: from bacteria to predators, from meadows to currents” granted by the Italian Ministry of University and Research (MUR) under the National Recovery and Resilience Plan (NRRP) funded by the European Union - NextGenerationEU (MUR Prin PNRR 2023, project code P202254HT8, Grant No. CUP B53D23027760001);
- PNRR MUR - M4C2 Project, grant number N00000013 - CUP D93C22000430001;
- the INdAM-GNCS Project CUP - E53C23001670001.
- PRIN2022PNRR n. verb+P2022M7JZW+ “*SAFER MESH - Sustainable mAnagement oF watEr Resources ModElS and numerical MethOds*” research grant, funded by the Italian Ministry of Universities and Research (MUR) and by the European Union through Next Generation EU, M4C2.

## References

- [1] N. Asano, Y. Kato, Algebraic and spectral methods for nonlinear wave equations, volume 49, Longman Scientific and Technical, 1990.
- [2] Z.-f. Liang, X.-y. Tang, W. Ding, Infinitely many nonlocal symmetries and nonlocal conservation laws of the integrable modified kdv-sine-gordon equation, Communications in Theoretical Physics 73 (2021) 055003.
- [3] G. Wang, A novel  $(3+1)$ -dimensional sine-gordon and a sinh-gordon equation: derivation, symmetries and conservation laws, Applied Mathematics Letters 113 (2021) 106768.
- [4] H. Blas, H. F. Callisaya, J. Campos, Riccati-type pseudo-potentials, conservation laws and solitons of deformed sine-gordon models, Nuclear Physics B 950 (2020) 114852.
- [5] P. Miškinis, The nonlinear and nonlocal integrable sine-gordon equation, Mathematical Modelling and Analysis 10 (2005) 367–376.

- [6] G. Alfimov, V. Eleonsky, L. Lerman, Solitary wave solutions of nonlocal sine-gordon equations, *Chaos: An Interdisciplinary Journal of Nonlinear Science* 8 (1998) 257–271.
- [7] J.-y. Wang, X.-y. Tang, Z.-f. Liang, S.-y. Lou, Infinitely many nonlocal symmetries and conservation laws for the  $(1+1)$ -dimensional sine-gordon equation, *Journal of Mathematical Analysis and Applications* 421 (2015) 685–696.
- [8] G. Alfimov, T. Pierantozzi, L. Vázquez, Numerical study of a nonlocal sine-gordon equation, in: *Nonlinear Waves: Classical and Quantum Aspects*, Springer, 2005, pp. 121–128.
- [9] X.-y. Tang, Z.-f. Liang, J.-y. Wang, Nonlocal topological solitons of the sine-gordon equation, *Journal of Physics A: Mathematical and Theoretical* 48 (2015) 285204.
- [10] X.-b. Xiang, W. Feng, S.-l. Zhao, Local and nonlocal complex discrete sine-gordon equation. solutions and continuum limits, *Theoretical and Mathematical Physics* 211 (2022) 758–774.
- [11] S. A. Silling, Reformulation of elasticity theory for discontinuities and long-range forces, *J. Mech. Phys. Solids* 48 (2000) 175–209. URL: [https://doi.org/10.1016/S0022-5096\(99\)00029-0](https://doi.org/10.1016/S0022-5096(99)00029-0). doi:10.1016/S0022-5096(99)00029-0.
- [12] S. A. Silling, Linearized theory of peridynamic states, *J. Elasticity* 99 (2010) 85–111. URL: <https://doi.org/10.1007/s10659-009-9234-0>. doi:10.1007/s10659-009-9234-0.
- [13] Q. Du, Y. Tao, X. Tian, A peridynamic model of fracture mechanics with bond-breaking, *J. Elasticity* 132 (2018) 197–218. URL: <https://doi.org/10.1007/s10659-017-9661-2>. doi:10.1007/s10659-017-9661-2.
- [14] E. Emmrich, D. Puhst, Measure-valued and weak solutions to the nonlinear peridynamic model in nonlocal elastodynamics, *Nonlinearity* 28 (2015) 285–307. URL: <https://doi.org/10.1088/0951-7715/28/1/285>. doi:10.1088/0951-7715/28/1/285.
- [15] A. C. Eringen, D. G. B. Edelen, On nonlocal elasticity, *Internat. J. Engrg. Sci.* 10 (1972) 233–248. URL: [https://doi.org/10.1016/0020-7225\(72\)90039-0](https://doi.org/10.1016/0020-7225(72)90039-0). doi:10.1016/0020-7225(72)90039-0.

- [16] E. Kröner, Elasticity theory of materials with long range cohesive forces, *International Journal of Solids and Structures* 3 (1967) 731–742. URL: <https://www.sciencedirect.com/science/article/pii/0020768367900492>. doi:[https://doi.org/10.1016/0020-7683\(67\)90049-2](https://doi.org/10.1016/0020-7683(67)90049-2).
- [17] S. Silling, R. Lehoucq, Peridynamic theory of solid mechanics, in: H. Aref, E. van der Giessen (Eds.), *Advances in Applied Mechanics*, volume 44 of *Advances in Applied Mechanics*, Elsevier, 2010, pp. 73–168. URL: <https://www.sciencedirect.com/science/article/pii/S0065215610440028>. doi:[https://doi.org/10.1016/S0065-2156\(10\)44002-8](https://doi.org/10.1016/S0065-2156(10)44002-8).
- [18] S. A. Silling, Linearized theory of peridynamic states, *J. Elasticity* 99 (2010) 85–111. URL: <https://doi.org/10.1007/s10659-009-9234-0>. doi:10.1007/s10659-009-9234-0.
- [19] S. A. Silling, M. Epton, O. Weckner, J. Xu, E. Askari, Peridynamic states and constitutive modeling, *J. Elasticity* 88 (2007) 151–184. URL: <https://doi.org/10.1007/s10659-007-9125-1>. doi:10.1007/s10659-007-9125-1.
- [20] S. A. Silling, R. B. Lehoucq, Convergence of peridynamics to classical elasticity theory, *J. Elasticity* 93 (2008) 13–37. URL: <https://doi.org/10.1007/s10659-008-9163-3>. doi:10.1007/s10659-008-9163-3.
- [21] G. M. Coclite, S. Dipierro, G. Fanizza, F. Maddalena, M. Romano, E. Valdinoci, Qualitative aspects in nonlocal dynamics, *Journal of Peridynamics and Nonlocal Modeling* (2021). URL: <https://doi.org/10.1007/2Fs42102-021-00064-z>. doi:10.1007/s42102-021-00064-z.
- [22] G. M. Coclite, S. Dipierro, G. Fanizza, F. Maddalena, E. Valdinoci, Dispersive effects in a scalar nonlocal wave equation inspired by peridynamics, *Nonlinearity* 35 (2022) 5664. URL: <https://dx.doi.org/10.1088/1361-6544/ac8fd9>. doi:10.1088/1361-6544/ac8fd9.
- [23] A. Coclite, G. M. Coclite, G. Fanizza, F. Maddalena, Dispersive effects in two- and three-dimensional peridynamics, *Acta Applicandae Mathematicae* 187 (2023) 13. URL: <https://doi.org/10.1007/s10440-023-00606-1>. doi:10.1007/s10440-023-00606-1.

- [24] R. Lipton, Dynamic brittle fracture as a small horizon limit of peridynamics, *Journal of Elasticity* 117 (2014) 21–50.
- [25] R. Lipton, Cohesive dynamics and brittle fracture, *Journal of Elasticity* 124 (2016) 143–191.
- [26] P. K. Jha, R. Lipton, Numerical analysis of nonlocal fracture models in hölder space, *SIAM Journal on Numerical Analysis* 56 (2018) 906–941. URL: <https://doi.org/10.1137/17M1112236>. doi:10.1137/17M1112236.
- [27] P. K. Jha, R. Lipton, Numerical convergence of finite difference approximations for state based peridynamic fracture models, *Computer Methods in Applied Mechanics and Engineering* 351 (2019) 184–225.
- [28] P. Jha, R. Lipton, Finite element approximation of nonlocal dynamic fracture models, *Discrete & Continuous Dynamical Systems-B* 26 (2021) 1675.
- [29] R. P. Lipton, P. K. Jha, Nonlocal elastodynamics and fracture, *Nonlinear Differential Equations and Applications NoDEA* 28 (2021) 1–44.
- [30] A. Coclite, G. M. Coclite, F. Maddalena, T. Politi, A numerical framework for nonlinear peridynamics on two-dimensional manifolds based on implicit  $p\text{-}(ec)^k$  schemes, *SIAM Journal on Numerical Analysis* 62 (2024) 622–645. URL: <https://epubs.siam.org/doi/abs/10.1137/22M1498942>. doi:10.1137/22M1498942.
- [31] S. A. Silling, E. Askari, A meshfree method based on the peridynamic model of solid mechanics, *Computers & structures* 83 (2005) 1526–1535.
- [32] X. Gu, Q. Zhang, X. Xia, Voronoi-based peridynamics and cracking analysis with adaptive refinement, *International Journal for Numerical Methods in Engineering* 112 (2017) 2087–2109.
- [33] M. Bessa, J. Foster, T. Belytschko, W. K. Liu, A meshfree unification: reproducing kernel peridynamics, *Computational Mechanics* 53 (2014) 1251–1264.
- [34] A. Shojaei, A. Hermann, C. J. Cyron, P. Seleson, S. A. Silling, A hybrid meshfree discretization to improve the numerical performance of peridynamic models, *Computer Methods in Applied Mechanics and Engineering* 391 (2022) 114544.

- [35] S. Jafarzadeh, A. Larios, F. Bobaru, Efficient solutions for nonlocal diffusion problems via boundary-adapted spectral methods, *Journal of Peridynamics and Nonlocal Modeling* 2 (2020) 85–110.
- [36] L. Lopez, S. F. Pellegrino, A spectral method with volume penalization for a nonlinear peridynamic model, *International Journal for Numerical Methods in Engineering* 122 (2021) 707–725. doi:<https://doi.org/10.1002/nme.6555>.
- [37] L. Lopez, S. F. Pellegrino, A space-time discretization of a nonlinear peridynamic model on a 2D lamina, *Computers and Mathematics with Applications* 116 (2022) 161–175. doi:<https://doi.org/10.1016/j.camwa.2021.07.004>.
- [38] L. Lopez, S. F. Pellegrino, A fast-convolution based space-time Chebyshev spectral method for peridynamic models, *Advances in Continuous and Discrete Models* 70 (2022). URL: <https://doi.org/10.1186/s13662-022-03738-0>. doi:<https://doi.org/10.1186/s13662-022-03738-0>.
- [39] L. Lopez, S. F. Pellegrino, A non-periodic Chebyshev spectral method avoiding penalization techniques for a class of nonlinear peridynamic models, *International Journal for Numerical Methods in Engineering* 123 (2022) 4859–4876. doi:<https://doi.org/10.1002/nme.7058>.
- [40] L. Lopez, S. F. Pellegrino, Computation of Eigenvalues for Nonlocal Models by Spectral Methods, *Journal of Peridynamics and Nonlocal Modeling* 5 (2023) 133–154. URL: <https://doi.org/10.1007/s42102-021-00069-8>. doi:10.1007/s42102-021-00069-8.
- [41] X. Liang, L. Wang, J. Xu, J. Wang, The boundary element method of peridynamics, *International Journal for Numerical Methods in Engineering* 122 (2021) 5558–5593.
- [42] N. Dimola, A. Coclite, G. Fanizza, T. Politi, Bond-based peridynamics, a survey prospecting nonlocal theories of fluid-dynamics, *Adv. Contin. Discrete Models* 2022 (2022) 26. doi:10.1186/s13662-022-03732-6, id/No 60.
- [43] G. M. Coclite, S. Dipierro, F. Maddalena, E. Valdinoci, Wellposedness of a nonlinear peridynamic model, *Nonlinearity* 32 (2018) 1–21. URL: <http://dx.doi.org/10.1088/1361-6544/aae71b>. doi:10.1088/1361-6544/aae71b.

- [44] G. M. Coclite, S. Dipierro, F. Maddalena, G. Orlando, E. Valdinoci, Comparison between solutions to the linear peridynamics model and solutions to the classical wave equation, 2024. URL: <https://arxiv.org/abs/2410.09211>. arXiv:2410.09211.
- [45] G. El, L. Nguyen, N. F. Smyth, Dispersive shock waves in systems with nonlocal dispersion of benjamin–ono type, *Nonlinearity* 31 (2018) 1392.
- [46] L. T. K. Nguyen, N. F. Smyth, Dispersive shock waves for the boussinesq benjamin–ono equation, *Studies in Applied Mathematics* 147 (2021) 32–59.
- [47] C. Canuto, Boundary Conditions in Chebyshev and Legendre Methods, *SIAM Journal on Numerical Analysis* 23 (1986) 815–831. doi:<https://doi.org/10.1137/0723052>.
- [48] L. N. Trefethen, *Spectral Methods in MATLAB*, Society for Industrial and Applied Mathematics, 2000. URL: <https://epubs.siam.org/doi/abs/10.1137/1.9780898719598>. doi:10.1137/1.9780898719598. arXiv:<https://epubs.siam.org/doi/pdf/10.1137/1.9780898719598>.
- [49] C. Canuto, A. Quarteroni, Approximation results for orthogonal polynomials in Sobolev spaces, *Math. Comp.* 38 (1982) 67–86. doi:<https://doi.org/10.1090/S0025-5718-1982-0637287-3>.
- [50] S. Bilbao, M. Ducceschi, F. Zama, Explicit exactly energy-conserving methods for Hamiltonian systems, *Journal of Computational Physics* 472 (2023) 111697.
- [51] E. Hairer, C. Lubich, G. Wanner, Geometric numerical integration illustrated by the Störmer-Verlet method, *Acta Numerica* 12 (2003) 399 – 450. doi:<https://doi.org/10.1017/S0962492902000144>.